5248 J. Med. Chem. 2010, 53, 5248–5255
DOI: 10.1021/jm100198t

Journal of Medicinal Chemistry Article

Click Chemistry Approach to New N-Substituted Aminocyclitols as Potential Pharmacological Chaperones for Gaucher Disease†

Lucía Díaz,‡ Jordi Bujons,‖ Josefina Casas,§ Amadeu Llebaria,§ and Antonio Delgado*,‡,§

‡Facultat de Farmàcia, Unitat de Química Farmacèutica (Unitat Associada al CSIC), Universitat de Barcelona, Avda. Joan XXIII, s/n, 08028 Barcelona, Spain, §Research Unit on Bioactive Molecules (RUBAM), Departament de Química Biomèdica, Institut de Química Avançada de Catalunya (IQAC-CSIC, Spanish National Research Council), Jordi Girona 18-26, 08034 Barcelona, Spain, and ‖Department de Química Biològica i Modelització Molecular, Institut de Química Avançada de Catalunya (IQAC-CSIC, Spanish National Research Council), Jordi Girona 18-26, 08034 Barcelona, Spain

Received February 15, 2010

New *N*-alkylaminocyclitols bearing a 1,2,3-triazole system at different positions of the alkyl chain have been prepared as potential GCase pharmacological chaperones using click chemistry approaches. Among them, compounds **1d** and **1e**, with the shorter spacer ($n = 1$) between the alkyltriazolyl system and the aminocyclitol core, were the most active ones as GCase inhibitors, revealing a determinant effect of the location of the triazole ring on the activity. Furthermore, SAR data and computational docking models indicate a correlation between lipophilicity and enzyme inhibition and suggest "extended" and "bent" potential binding modes for the compounds. In the "bent" mode, the most active compounds could establish a hydrogen-bond interaction between the triazole moiety and enzyme residue Q284. Such an interaction would be precluded in compounds with a longer spacer between the triazole and the aminocyclitol core.

Introduction

Gaucher disease is one of the most prevalent lysosomal storage disorders characterized by the accumulation of the sphingolipid glucosylceramide in the lysosomes. The disease is caused by the deficient activity elicited by several mutated forms of the enzyme glucocerebrosidase (GCase[a]), the β-glucosidase that hydrolyzes glucosylceramide into glucose and ceramide.[1] Cellular levels of the mutated, misfolded enzyme are abnormally low because of its premature degradation by specific cytosolic endoproteases in the endoplasmic reticulum. Several therapeutic strategies for Gaucher disease have been developed over the past years.[2] Among them, the use of pharmacological chaperones, competitive inhibitors of the target enzyme that assist the proper folding of the defective protein at subinhibitory concentrations,[3−5] is an active field of research.[6] In this context, several iminosugars and aminocyclitols have been reported in the literature (Figure 1).

To date, a number of GCase structures in its native state[7] with different degrees of glycosylation,[8−10] under different pH conditions,[11,12] or as a complex with different inhibitors[13−16] have been reported. All these structures show a very similar 3D-arrangement for the protein with four loops (L1−L4) located at the entrance to the catalytic site that control open and closed conformations (see below). Differences on the surface topology of GCase close to the entrance to the active site have been observed in structures of the enzyme complexed with different inhibitors. Thus, while in *N*-nonyldeoxynojirimycin (NNDNJ) and *N*-butyldeoxynojirimycin (NBDNJ)−GCase complexes the *N*-alkyl chains are stabilized by accommodation into the hydrophobic valley between L3 and L4, an additional hydrophobic groove between L1 and L3 is observed in the isofagomine (IFG)−GCase complex structure.[14,15] Interestingly, these two valleys between L3 and L4 and between L1 and L3 have been modeled as possible binding locations for the two alkyl chains of the ceramide moiety in the natural substrate.[15]

Over the past years, we have been working actively on the development of new aminocyclitols with potential applicability

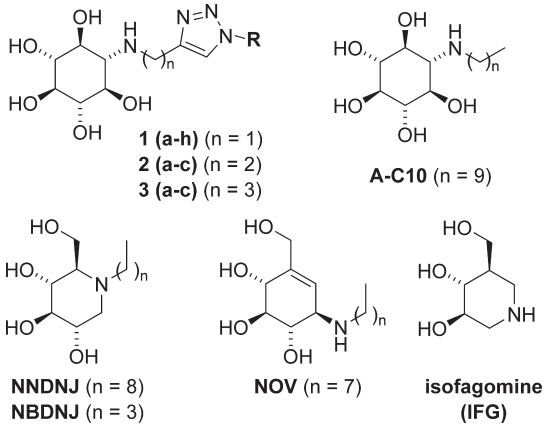

Figure 1. Aminocyclitols reported in this study (**1**−**3**), together with representative iminosugars and aminocyclitols reported as GCase inhibitors.

†Dedicated to Prof. Pelayo Camps on the occasion of his 65th anniversary.

*To whom correspondence should be addressed. Phone: +34-934006108. Fax: +34-932045904. E-mail: adelgado@cid.csic.es.

[a] Abbreviations: A-C10, *N*-decylaminocyclitol; CC_{50}, cytotoxic concentration for 50% of the cell population under study; clogP, calculated logarithm of the partition coeficient; GCase, β-glucocerebrosidase; IFG, isofagomine; NBDNJ, *N*-butyldeoxynojirimycin; NNDNJ, *N*-nonyldeoxynojirimycin ; NOV, *N*-octylvalienamine; SAR, structure−activity relationship.

 Published on Web 06/17/2010

Table 1. Aminocyclitols Arising from Click Chemistry Reaction between ω-Alkynyl Alkylaminocyclitols and Azides[a]

alkyne	azide (RN_3)	R (in RN_3)	click adduct	aminocyclitol
5	**23**	*n*-butyl	**10a**	**1a**
5	**25**	*n*-octyl	**10b**	**1b**
5	**26**	*n*-nonyl	**10c**	**1c**
5	**27**	*n*-decyl	**10d**	**1d**
5	**29**	*n*-dodecyl	**10e**	**1e**
5	**30**	*n*-tetradecyl	**10f**	**1f**
5	**31**	6-(propoxy)hexyl	**10g**	**1g**
5	**32**	2-phenylethyl	**10h**	**1h**
7	**25**	*n*-octyl	**11a**	**2a**
7	**26**	*n*-nonyl	**11b**	**2b**
7	**28**	*n*-undecyl	**11c**	**2c**
9	**24**	*n*-hexyl	**12a**	**3a**
9	**25**	*n*-octyl	**12b**	**3b**
9	**27**	*n*-decyl	**12c**	**3c**

[a] See Scheme 3.

as chemical chaperones of the enzyme GCase.[17,18] In our previous work, we found that aminocyclitol A-C10 (Figure 1), which stabilized GCase under thermal denaturation conditions[19] and inhibited GCase in wild type fibroblasts, behaved as a pharmacological chaperone in Gaucher disease patient fibroblasts bearing the L444P/G202R and L444P;E326K/G202R genotypes.[20] However, exploration of the chemical diversity around the amino group has met with limited success so far.[21] Thus, the most promising results arose from the regio- and stereoselective opening[22,23] of conduritol B epoxide with a series of aliphatic amines of different chain lengths.[19] In order to explore the role of the aminoalkyl side chain on the enzyme stabilization under thermal denaturation conditions,[24] a fast and convenient methodology aimed at the parallel synthesis of small to medium sized libraries of N-substituted aminocyclitol derivatives would be desirable. In this context, click-chemistry approaches based on the Cu-catalyzed 1,3-dipolar Huisgen cycloaddition of alkynes and azides are being widely used in drug design.[25,26] However, the electronic properties of the resulting 1,2,3-triazole system make possible the operation of additional interactions of uncertain effects at the active site level. In order to unravel such effects, we have synthesized and tested a small collection of *N*-alkylaminocyclitols arising from the formal placement of the triazole ring along the *N*-alkyl side chain. From a structural standpoint, the aminocyclitols presented in this study can be grouped into three different subsets (**1**−**3**) as a function of the spacer length (n = 1−3) between the aminocyclitol core and the triazole system (Figure 1).

Synthesis

Aminocyclitols **1**−**3** were obtained by the Cu-catalyzed 1,3-dipolar cycloaddition (Huisgen reation) of ω-alkynylaminocyclitols **5** (n = 1), **7** (n = 2), and **9** (n = 3) with a set of azides **23**−**32**, followed by massive benzyl removal (see Scheme 3 and Table 1).

Aminocyclitols **5**, **7**, and **9** were obtained, in turn, by the regio- and diastereoselective opening[22] of epoxide **4** with the commercially available propargylamine or amines **20** and **22**, followed by TMS removal (Schemes 1 and 2). The use of the TMS protecting group in amines **20** and **22** increased their boiling point, thus favoring their isolation, purification, and subsequent manipulation.

Copper-catalyzed Huisgen cycloaddition reaction of scaffolds **5**, **7**, and **9** with the aliphatic azides shown in Table 1

Scheme 1[a]

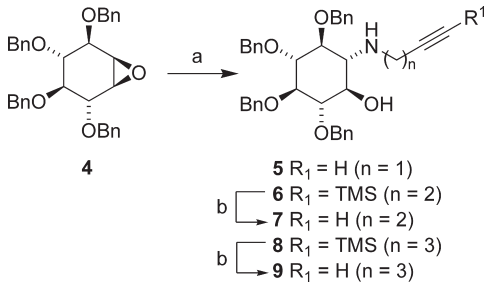

[a] Reagents and conditions: (a) amine (propargylamine, **20**, or **22**), $LiClO_4$, CH_3CN; (b) KF, DMSO.

afforded the expected fully benzylated triazolylalkylaminocyclitols **10**−**12** (Scheme 3). Massive *O*-benzyl deprotection was carried out either by hydrogenolysis or by reaction with BCl_3, following reported protocols.[17,27]

Results and Discussion

A pharmacological chaperone binds to the active site of the target enzyme at the neutral pH of the endoplasmic reticulum (ER) to assist in protein folding and also to enhance the enzyme transport to lysosomes. However, it partly dissociates at the low pH of the lysosomal environment while still stabilizing the enzyme at that acidic pH. Consequently, compounds were evaluated as inhibitors of recombinant GCase (imiglucerase (Cerezyme)) at both neutral and acidic pH. Compounds **1**, bearing the shorter spacer (n = 1) (see Tables 1 and 2) gave IC_{50} values lower than those of compounds **2** and **3**, with a longer spacer (n = 2 and 3, respectively), resulting from the formal placement of the triazole ring along the aliphatic chain (compare the couples **1b**/**3a** and **1c**/**2a** and the triplets **1d**/**2b**/**3b** and **1e**/**2c**/**3c**). Inhibition constants (K_i) for the most active compounds in each series showed, in all cases, a competitive inhibition pattern, as illustrated in Figure 2 for **1d** (Table 2).[28]

It is worth mentioning that the low K_i values found for compounds **1d**−**1f** were in the 60−90 nM range. Interestingly, none of the above aminocyclitols showed significant activity on glucosyl ceramide synthase (GCS) from cell homogenates at 250 μM, thus indicating a selectivity toward the hydrolytic enzyme.[29] Moreover, the above aminocyclitols were inactive at 0.1 mM against a panel of commercially available α- and β-glycosidases,[30] reinforcing the selectivity against GCase.

Regarding neutral pH, IC_{50} values for compounds **1** were similar to or slightly lower than those at acidic pH, with the exception of **1e** and **1h** (Table 2). Interestingly, compounds **2** and **3** showed lower IC_{50} values at neutral pH, an indication of the ability of the inhibitors to interact with the enzyme at the cellular pH of both ER and lysosomes.

Enzyme stabilization under thermal denaturation conditions, expressed as the stabilization ratio (see Table 2), was used as an indication of the potential of the target compounds to behave as pharmacological chaperones.[24] An IC_{50} threshold of 15 μM at pH 7.4 was set as selection criteria for the thermal stabilization assay. Recovery of GCase activity was measured at 48 °C in the presence and in the absence of increasing concentrations (from 0.50 to 150 μM or from 50 to 150 μM, as appropriate) of selected aminocyclitols at different incubation times (Figure 3). For comparative purposes, NNDNJ and our previously reported aminocyclitol A-C10[19] (Figure 1) were also assayed under the same experimental conditions.

Scheme 2. Synthesis of Amines[a]

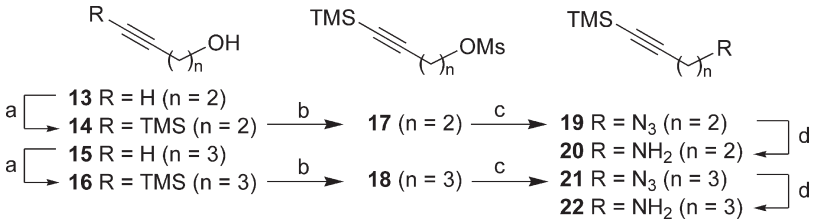

[a] Reagents and conditions: (a) TMSCl, BuLi, THF, −78 °C; (b) MsCl, Et_3N, THF, 0 °C; (c) NaN_3, DMF; (d) $LiAlH_4$, THF.

Scheme 3[a]

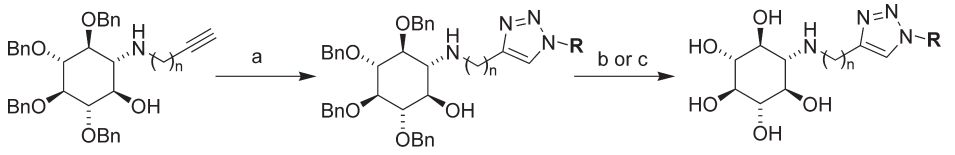

5 (n = 1)
7 (n = 2)
9 (n = 3)

10 (a-h) (n = 1)
11 (a-c) (n = 2)
12 (a-c) (n = 3)

1 (a-h) (n = 1)
2 (a-c) (n = 2)
3 (a-c) (n = 3)

[a] Reagents and conditions: (a) R-N_3 (**23**−**32**; see Table 1), Cu_2SO_4, sodium ascorbate, H_2O/THF (1:1); (b) BCl_3, CH_2Cl_2 (−78 °C); (c) H_2, Pd/C.

Table 2. Inhibitory Activity of Aminocyclitols **1a**−**h**, **2a**−**c**, and **3a**−**c** against Imiglucerase[a]

	IC_{50} (μM)				
compd	pH 7.4	pH 5.2	K_i (μM)[b]	stabilization ratio[c,d]	% inhibition GCase in human wt fibroblasts[e]
1a	nd	178	nd	nd	< 5
1b	1.1	1.0	1.8	1.0	20
1c	0.20	0.20	0.33	13.0	50
1d	0.09	0.10	0.09	21.0	90/71[f]/58[g]
1e	0.06	0.03	0.06	28.7	*h*/90[f] /87[g]
1f	0.10	0.09	0.08	13.2	*h*, *i*/93[g]
1g	6.2	7.4	2.4	1.1	< 5
1h	25.0	10.8	19.1	nd	< 5
2a	55.9	167	nd	nd	< 5
2b	11.0	44.7	nd	7.6	< 5
2c	4.9	25.4	20.2	11.6	50
3a	44.6	257	nd	nd	< 5
3b	18.2	35.4	19.9	nd	40
3c	1.2	3.5	7.6	1.4	20
NNDNJ	0.30	1.3, 0.66[j]	0.30[j]	9.2	nd
A-C10		1.8	0.30	4.9	nd

[a] See also Table 1 and Scheme 3 for structures). nd: not determined. [b] Competitive inhibitors (determined at pH 5.2). [c] Defined as the ratio of relative enzymatic activities (inhibitor vs control) at a given inhibitor concentration and incubation time. Tabulated values for 100 μM inhibitor and 60 min of incubation time. [d] See also Supporting Information. [e] Incubation for 24 h at 50 μM inhibitor and 5 mM substrate. [f] Incubation for 24 h at 20 μM inhibitor and 5 mM substrate. [g] Incubation for 24 h at 10 μM inhibitor and 5 mM substrate. [h] Toxic at 50 μM. [i] Toxic at 20 μM. [j] According to Compain et al. *ChemBioChem* **2006**, *7*, 1356−1359.

Among the compounds tested as GCase stabilizers, compounds **1b**, **1g**, and **3c** exhibited a similar, albeit almost negligible, activity pattern at the different times and concentrations tested. On the other hand, compounds **1c**, **1f**, **2b**, and **2c** showed an enzyme stabilization profile comparable to or even superior to that of NNDNJ, with stabilization ratios between 7.6 and 13.2 at 100 μM after 1 h of incubation time at 48 °C (Table 2 and Figure 3A). This parameter was even higher for aminocyclitols **1d** and **1e**, with values ranging from 20 to 30 at the above concentrations and incubation times. Compounds **1d** and **1e** were also assayed at lower concentrations (0.5−25 μM), showing a good correlation between the stabilization ratio and the concentration used in the experiment (Figure 3B and Supporting Information). Interestingly, enzyme thermal stabilization correlates well with K_i values in compounds **1a**−**h**, while most of the aminocyclitols tested in this study were not cytotoxic in wild type human fibroblasts at concentrations up to 300 μM.[31]

Finally, some of the aminocyclitols also behaved as GCase inhibitors in wild type human fibroblasts after 24 h of incubation at 50 μM (Table 2). A good correlation between K_i and GCase inhibition was observed for compounds **1b**−**d** in this assay. Since compounds **1e** and **1f** could not be tested at the above concentration because of their toxicity,[31] they were tested at 20 and 10 μM, together with **1d** for the sake of comparison (Table 2). Interestingly, compound **1e** was an even better inhibitor than **1d** at 20 μM and almost equipotent to **1f** at 10 μM. However, the high efficacy of **1d**,[31] together with its acceptable biological profile, low toxicity, and high enzyme affinity and enzyme thermal stabilization properties, makes this compound a promising candidate for further studies.

Activity data for the compounds described in this work reflect a clear dependence between GCase inhibition and clogP (see Supporting Information). Thus, in each series, activity increases with hydrophobicity, as shown in Figure 4. An exception to this trend is found for compound **1f**, with the longest *N*-triazolylalkyl chain (C_{14}) and the highest clogP value, which shows the same or lower activity than its less hydrophobic and shorter homologues **1d** (C_{10}) and **1e** (C_{12}). It is noteworthy that compounds **1e** and **1f** are toxic at high concentrations (>50 μM) and that this has also been observed for other analogues containing highly hydrophobic moieties,[19] which suggests a lipophilicity-related toxic effect. Furthermore, since the activity of aminocyclitols with *N*-alkyltriazolylalkyl chains of identical combined length is higher for compounds with the shortest spacer ($n = 1$, Figure 1) between the aminocyclitol and the triazole moieties (see above), a restriction to the length of the *N*-triazolylalkyl chain R and to the position of the triazole ring for optimum binding to the enzyme can be envisaged. Therefore, docking studies were

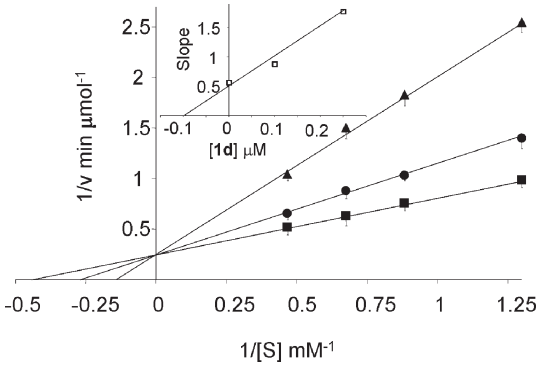

Figure 2. Type of inhibition of glucocerebrosidase by **1d**. Double reciprocal plot of imiglucerase incubated at different concentrations of substrate and compound **1d** (square, 0 μM; circle, 0.1 μM; triangle, 0.25 μM). Regression lines arise from data obtained in two different experiments with triplicates.

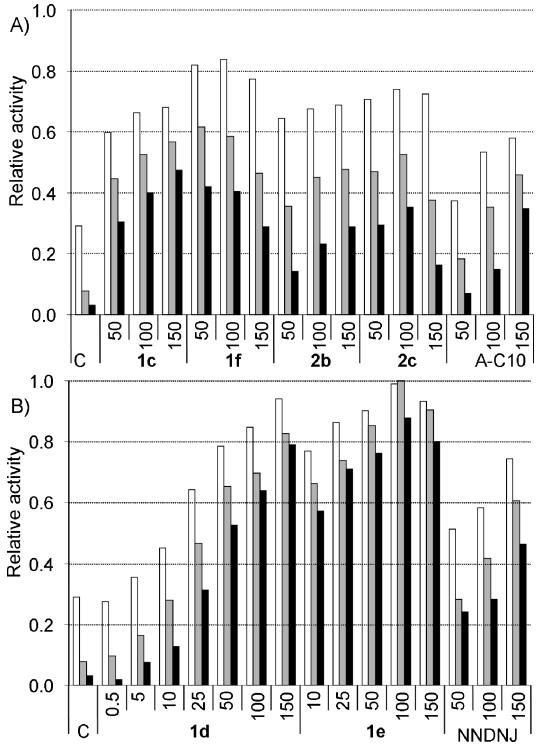

Figure 3. (A) and (B) Relative enzymatic activity after thermal denaturation (48 °C) for 20 min (white bar), 40 min (gray bar), and 60 (black bar) at the indicated inhibitor concentrations (μM) compared to the corresponding assay at 37 °C. Data for control (C) are obtained as above except that no inhibitor is present.

conducted to shed light on the way of binding of the aminocyclitols described in this work to the active center of GCase.

In order to explore all the potential binding modes of compounds **1**−**3**, the structures of the GCase−inhibitor complexes with NNDNJ (PDB code 2V3E, Figure 5A), IFG (PDB code 2NSX, Figure 5B), and NBDNJ (PDB code 2V3D, Supporting Information) were chosen as target structures for docking. Parts C and D of Figure 5 show the best docked conformations obtained using the 2V3E and 2NSX structures, respectively, as targets. The results obtained with the 2V3D structure were similar to those shown in Figure 5C (see Supporting Information). In the docked poses obtained using the NNDNJ−GCase complex (Figure 5C), the cyclitol moiety is

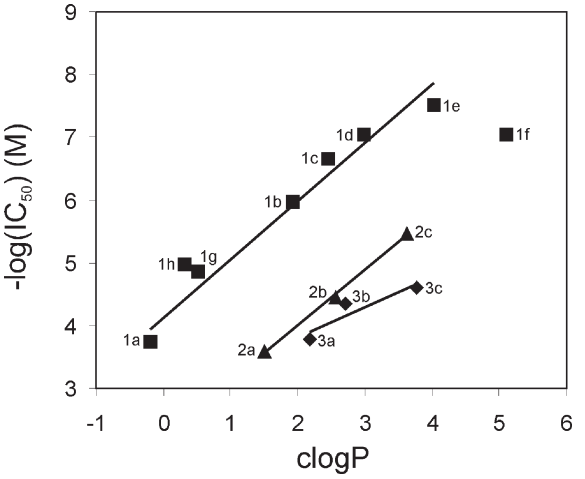

Figure 4. GCase inhibitory activity, expressed as $-\log(IC_{50})$, vs clogP for compounds of series **1**−**3**.

placed inside the GCase active site and the triazole and alkyl chain moieties adopt an "extended" conformation on the exposed surface of the enzyme between loops 3 and 4. The results obtained using the IFG−GCase structure (Figure 5D), however, showed an alternative binding mode for most of the compounds in which the cyclitol moiety still occupies the active site of the enzyme, but the triazole and the alkyl chain adopt a "bent" conformation to reach the narrow groove between loops 1 and 3. Parts E and F of Figure 5 show the best poses obtained for compound **1d** docked against 2V3E and 2NSX, respectively, and illustrates the main interactions between this compound and the protein in each particular conformation (corresponding interaction diagrams in Supporting Information). Similar interactions were observed for the analogue compounds **1e** and **1f**.

Hence, the best pose obtained for **1d** docked against structure 2V3E (Figure 5E) shows the hydroxyl groups of the cyclitol moiety establishing hydrogen bonds with residues D127, W179, W381, and N396. An additional strong interaction between the charged nitrogen atom of **1d** and the carboxylate group of E235 is observed. The charge on this nitrogen is also stabilized by a π−cation interaction with Y313. Finally, the "extended" alkyl chain is stabilized by less specific hydrophobic contacts with residues L240, L241, L286, L287, and L314. On the other hand, the best pose obtained for the same compound docked against structure 2NSX (Figure 5F) shows similar hydrogen bonding and polar interaction patterns, but the "bent" conformation of the alkyl moiety is now stabilized by hydrophobic interactions with residues W312, Y313, L314, and F316. Different poses obtained for compound **1d**, and also for the rest of the compounds studied, show slight variations in their binding mode to the different structures of GCase considered, which are most probably derived from the large flexibility of the alkyl substituents and from the high number of polar residues in the active site of GCase, which allows for alternative hydrogen bonding patterns.

Although obtaining a good correlation between docking scores and experimentally determined binding affinities is frequently not possible because of, inter alia, the limitations of scoring functions and sampling algorithms,[32,33] a reasonable correlation was obtained for the compounds in series **1** (n = 1) when the scores from docking to the structure of the "bent" IFG−GCase complex were considered (Figure 6). Since no such correlation was observed from the docking runs

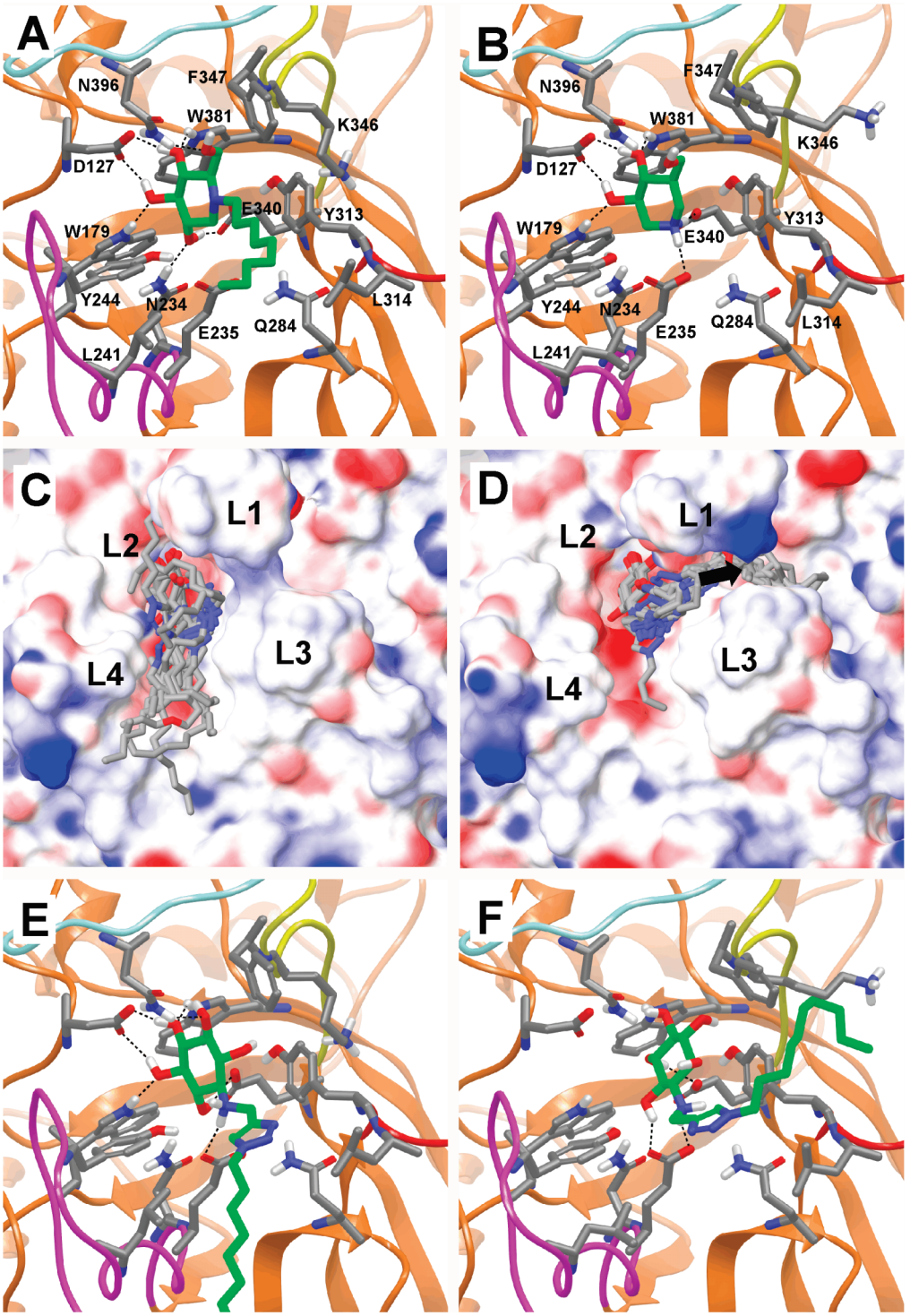

Figure 5. Crystal structures of (A) the NNDNJ−GCase complex (PDB 2V3E) and (B) the IFG−GCase complex (PDB 2NSX). Loops 1, 2, 3, and 4 (loop numbering based on ref 14) are colored in yellow, light blue, red, and purple, respectively. Best docked poses obtained for compounds **1**−**3** using structures 2V3E (C) and 2NSX (D) as targets. The orientation of the protein structures is similar to that shown in panels A and B, respectively. L1, L2, L3, and L4 denote the position of loops 1−4. In panel D, a black arrow shows the accessible groove between loops 1 and 3. Best poses obtained for compound **1d** docked against structures 2V3E (E) and 2NSX (F) as targets.

with the "extended" NNDNJ−GCase complex (see docking scores in the Supporting Information), this suggests the "bent" mode of binding as the preferred one for compounds **1**. Compounds of series **2** and **3** also followed an approximate linear dependence between both calculated and experimental parameters, similar to that observed when hydrophobicity was considered (Figure 4). However, these docking results do not clarify the role of the triazole moiety in the binding process, since no clear difference in the binding mode among the three series (spacer n = 1−3, Figure 1) was observed and no clear interaction between the triazole ring and the receptor was detected in any case. In this context, the triazole group has been considered as a good amide bond mimic, being able to act as a hydrogen bond acceptor.[34−36]

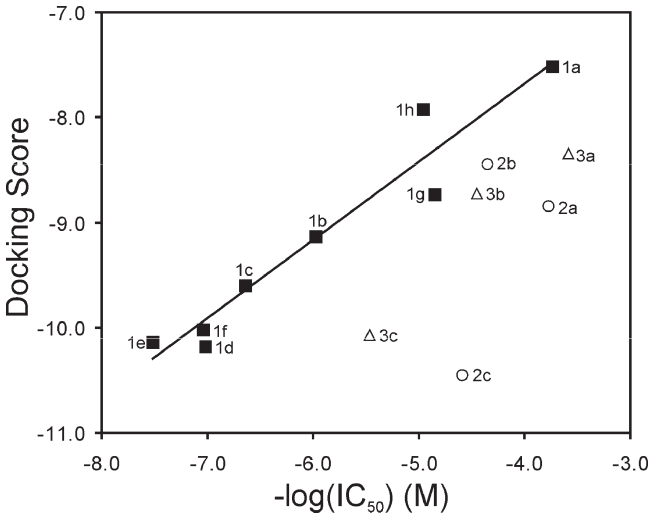

Figure 6. Correlation of docking scores vs experimentally determined $-\log(IC_{50})$ values for compounds **1**−**3** docked against IFG−GCase complex (structure 2NSX).

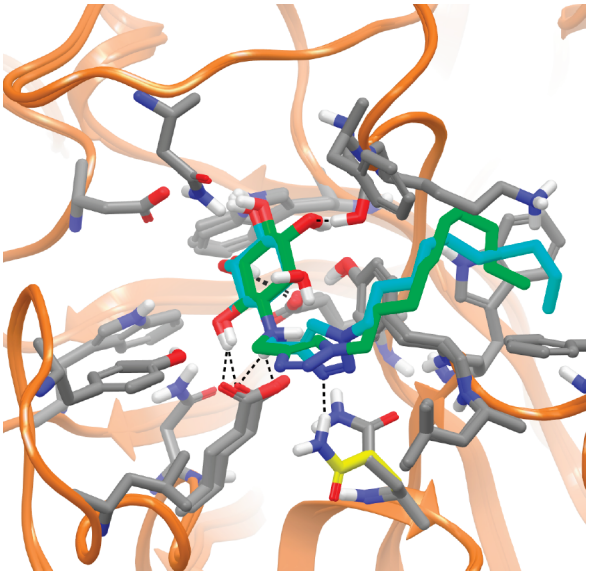

Figure 7. Best pose obtained for compound **1d** when docked into the active site of structure 2NSX (green) and pose obtained after minimization allowing receptor flexibility (cyan), which shows movement of the side chain of residue Q284 (yellow) and of the triazole ring, leading to the formation of a new hydrogen bond.

Minimization of some of the "bent" docking poses obtained for compound **1d**, as well as those of other analogs from series **1**, was carried out allowing for movement of the closest residues of the protein. Interestingly, the results showed that the Q284 side chain can rotate to form a new hydrogen bond with the triazole N3 nitrogen atom (Figure 7). Compounds of series **2** and **3**, having a longer spacer between the triazole and the cyclitol moieties, would require a larger movement of this residue, and perhaps others, to establish such an interaction. This might be energetically more expensive and would explain their lower affinity. Clearly, additional modeling studies are needed to verify such hypotheses and to understand how the triazole ring can influence the binding strength of these compounds.

Conclusion

New *N*-alkylaminocyclitols bearing a 1,2,3-triazole system at different positions of the alkyl chain have been prepared using click chemistry protocols. The resulting compounds have been tested as GCase inhibitors and also for their ability to increase the enzyme stability against thermal denaturation, as an in vitro assessment of their potential as pharmacological chaperones. Among them, compounds **1d** and **1e** have emerged as promising candidates for further development, in light of the comparative results with NNDNJ and our previously reported aminocyclitol A-C10.

In spite of the good correlation between lipophilicity and IC_{50} values, the position of the triazole system along the *N*-alkyl chain is crucial for enzyme inhibition and thermal stabilization, since members with the shorter spacer between the aminocyclitol core and the alkyltriazolyl system exhibited the maximum potency. Modeling studies using three different reported GCase−inhibitor complexes (PDB codes 2V3D, 2V3E, and 2NSX) showed two alternative modes of binding with an apparently preferred "bent" mode (based on docking scores) for the most active compounds of this study. Although the docking results do not clarify the role of the triazole moiety in this binding process, the accepted ability of triazole to act as a hydrogen bond acceptor would allow the operation of a new hydrogen bond between triazole N3 and amino acid Q284 by a slight rearrangement of the conformation of the side chain of this residue found in the crystal structure. This additional interaction would likely be precluded in compounds with a longer spacer (series **2** and **3**). Studies addressed at clarifying the role of triazole in these systems are currently underway in our group and will be published in due course.

Experimental Section

Chemistry: General Protocols. Solvents were distilled prior to use and dried by standard methods. FT-IR spectra are reported in cm^{-1}. ^1H and ^{13}CNMR spectra were obtained in $CDCl_3$ solutions at 300 MHz (for ^1H) and 75 MHz (for ^{13}C), respectively, unless otherwise indicated. Chemical shifts are reported in δ units, parts per million (ppm) relative to the singlet at 7.24 ppm of $CDCl_3$ for ^1H and in ppm relative to the center line of a triplet at 77.0 ppm of $CDCl_3$ for ^{13}C. ESI/HRMS spectra were recorded on a Waters LCT Premier mass spectrometer. Purity of compounds used for enzyme assays was ≥95%, as judged by HPLC analysis (Gemini C18 column, 4.6 mm × 250 mm, 5 μm) under the following chromatographic conditions: mobile phase A, water containing 0.1% v/v trifluoroacetic acid; mobile phase B, ACN containing 0.1% v/v trifluoroacetic acid; flow rate of 1.0 mL/min; detection, SATIN-ELS (evaporative light scattering) (λ = 254 nm); gradient elution, 0 min, from 80% A/20% B to 0% A/100% B over next 20 min. Each run was followed by a 3 min wash with 80% ACN, 20% water.

General Method for Click Reactions: Synthesis of 10e as Representative Example. A solution of the azide **29** (0.25 mmol) (see Table 1) in a mixture H_2O/THF (1:1) (2 mL) was added to aminocyclitol **5** (0.20 mmol) in a vial. Then $CuSO_4 \cdot 5H_2O$ (5.2 mg, 0.020 mmol) and a catalytic amount of sodium ascorbate were added. The mixture was stirred at room temperature for 2 min, quenched with water (3 mL), and extracted with EtOAc (3 × 5 mL). Usual workup afforded a green solid, which was purified by flash chromatography on elution with ethyl acetate. Compound **10e** was obtained in 60% yield. ^1H NMR (500 MHz, $CDCl_3$): 7.44 (m, 20, 1H), 4.92 (m, 8H), 4.30 (s, 2H), 4.11 (m, 2H), 3.56 (m, 5H), 2.69 (t, 1H), 1.88 (d, 2H, J = 1.2 Hz), 1.32 (m, 18H), 0.92 (t, 3H, J = 6.9 Hz). ^{13}C NMR (400 MHz, $CDCl_3$): 146.88, 138.72−138.37, 128.59−127.50, 121.21, 84.76, 84.10, 83.078, 81.85, 73.03, 61.54, 50.39, 43.12, 31.97- 29.11,

22.76, 14.22. HRMS calculated for $C_{49}H_{65}N_4O_5$ ($M + H^+$): 789.4955. Found: 789.4935.

Debenzylation with Boron Trichloride: Synthesis of 1e as Representative Example. A solution of **10e** (0.05 mmol) in CH_2Cl_2 (2 mL) under nitrogen at −78 °C was treated with 1 M BCl_3 solution in heptane (0.4 mL). After being stirred for 2 h at −78 °C, the reaction mixture was allowed to warm to room temperature and stirred for additional 12 h at room temperature. The mixture was next cooled to −78 °C, quenched with methanol (1 mL), and evaporated under reduced pressure. The resulting residue was taken up in a 1:1 MeOH/H_2O mixture, filtered through a small pad of charcoal, and evaporated to afford **1e** as the corresponding hydrochloride in 87% yield. ^{1}H NMR (500 MHz, CD_3OD): 8.24 (s, 1H), 4.63 (s, 2H), 4.47 (t, 2H, J = 7.1 Hz), 3.64 (m, 2H), 3.30 (m, 3H), 3.13 (t, 1H, J = 10.7 Hz), 1.94 (dd, 2H, J = 6.9 Hz, J = 13.8 Hz), 1.26 (m, 18H), 0.91 (t, 3H, J = 6.9 Hz). ^{13}C NMR (400 MHz, CD_3OD): 77.46, 76.06, 71.72, 63.98, 59.18, 42.89, 33.79, 32.02, 31.46, 31.39, 31.29, 31.15, 30.87, 28.29, 24.43, 21.28, 19.17, 15.1. Triazole ^{13}C signals were not observed in any of the click adducts because of unsuitable relaxation times. However, their presence was confirmed by a combination of gHSQC and gHMBC experiments from a representative library member (see Supporting Information for details). HRMS calculated for $C_{21}H_{41}N_4O_5$ ($M + H^+$): 429.3077. Found: 429.3014.

GCase Inhibition. In vitro activity was determined with 4 mM 4-methylumbelliferyl-β-D-glucopyranoside in McIlvaine buffer (pH 5.2 or 7.4). Enzyme solutions (25 μL from a stock solution containing 0.1 mg of protein/mL) in the presence of 0.2% (w/v) sodium taurocholate and 0.1% (v/v) Triton X-100 in McIlvaine buffer (pH 5.2 or 7.4) were incubated at 37 °C without (control) or with inhibitor (1 mM) during 30 min, and after addition of corresponding substrate solution (60 μL), incubations were maintained at 37 °C for 10 min. Enzymatic reactions were stopped by the addition of 150 μL of 100 mM glycine/NaOH buffer (pH 10.6). The amount of 4-methylumbelliferone formed was determined with a 1420 VICTOR^2 multilabel counter (Wallac) fluorometer at 355 nm (excitation) and 460 nm (emission).

IC_{50} values were determined by plotting percent activity versus log [I], using at least five different inhibitor concentrations. Type of inhibition and K_i values for more active inhibitors were determined by Lineweaver−Burk or Dixon plots of assays performed with different concentrations of inhibitor and substrate.

Thermal Stabilization Assay. Following a modification of a reported method,[37] GlcCerase aliquots (48 μL, 2 mg/mL) were incubated at pH 7.4 with 0 (control), 10, 25, 50, 100, or 150 μM test compound at 48 °C. Subsequently, 150 μL of 0.1 M acetate−phosphate buffer (pH 5.0) and 100 μL of substrate (4 mM 4-methyllumbelliferyl β-D-glucoside) in McIlvaine buffer (pH 5.2) were added at different times and incubated for 10 min at 37 °C in the presence of 0.1 % Triton X-100 and 0.2% taurodeoxycholic acid. Then an amount of 300 μL of glycine buffer (200 mM, pH 10.6) was added, and liberated 4-methylumbelliferone was measured. Enzyme activity was reported relative to that of the enzyme at 37 °C.

Computational Methods. All molecular simulations were conducted with the package Schrödinger Suite 2008 (Schrödinger LLC), through its graphical interphase Maestro.[38] The program Macromodel[39] with its default force field OPLS 2005, a modified version of the OPLS-AA force field,[40] and GB/SA water solvation conditions[41] were used for all energetic calculations. The program Glide[42−44] was used for the docking calculations using the default XP precision settings except for the following: (i) given the high flexibility of most of the compounds, a setting of 5 000 000 poses per ligand for the initial phase of docking and a scoring window of 500 for keeping initial poses were chosen; (ii) constraints were applied to maintain the cyclitol moiety of the ligands inside the catalytic cavity of the CCase structures (preliminary docking runs showed, as expected, that the best scored poses for all compounds always had the cyclitol placed in that location); (iii) up to 50 poses per ligand were kept for the postdocking minimization. Glide XP scores[45] were used to rank the resulting docked poses. pK_a calculations for compounds **1a**−**h**, **2a**−**c**, and **3a**−**c** were performed with the pK_a prediction module[46] included in Jaguar[47]with its default settings. The coordinates of the complexes of human GCase with different inhibitors bound in its active site, i.e., isofagomine (PDB 2NSX), NB-DNJ (PDB 2V3D), or NN-DNJ (PDB 2V3E), were obtained from the Protein Data Bank[48] at Brookhaven National Laboratory. The structures of the proteins were prepared using the Protein Preparation Wizard included in Maestro to remove the solvent molecules and ligands, adding hydrogens, setting protonation states, and minimizing the energy using the OPLS force field. Compounds **1a**−**h**, **2a**−**c**, and **3a**−**c** were built within Maestro and preoptimized before docking using the LigPrep[49] application included in the software. All ligands were docked with the secondary amine group in the protonated state based on the results from pK_a calculations (see Supporting Information) and the fact that preliminary docking runs always yielded poses where this amino group was located in a highly polar environment, close to the carboxylate of D235 residue, which would favor the protonated form of the amine. Interaction diagrams were built with MOE[50] for the best docked poses obtained for some of the inhibitors.

Acknowledgment. Partial financial support from the "Ministerio de Ciencia e Innovación", Spain (Project CTQ-2008-01426/BQU), and "Generalitat de Catalunya" (Grant 2009SGR-1072) is acknowledged. L.D. is grateful to CSIC for predoctoral research training support within the JAE-Predoc program. The authors thank Dr. Meritxell Egido-Gabas for technical assistance, Núria Guillem and Laura Planas for experimental contributions, Eva Dalmau for HRMS analysis, and Genzyme Corp. for a generous supply of imiglucerase (Cerezyme). Finally, the authors acknowledge the "Centre de Supercomputació de Catalunya" (CESCA) for allowing the use of its software and hardware resources.

Supporting Information Available: General experimental protocols and compound characterization, cytotoxicity, inhibition of GlcCerase (wt fibroblasts), GCS (cell homogenates), and commercial glycosidases, stabilization ratios for thermal denaturation studies, and predicted pK_a and best Glide XP docking scores obtained for compounds **1a**−**h**, **2a**−**c**, and **3a**−**c** docked against targets 2V3D, 2V3E, and 2NSX. This material is available free of charge via the Internet at http://pubs.acs.org.

References

(1) Brady, R. O. Gaucher's disease: past, present and future. *Baillieres Clin. Haematol.* **1997**, *10*, 621–634.
(2) Sawkar, A. R.; D'Haeze, W.; Kelly, J. W. Therapeutic strategies to ameliorate lysosomal storage disorders—a focus on Gaucher disease. *Cell. Mol. Life Sci.* **2006**, *63*, 1179–1192.
(3) Morello, J.-P.; Bouvier, M.; Petaja-Repo, U. E.; Bichet, D. G. Pharmacological chaperones: a new twist on receptor folding. *Trends Pharmacol. Sci.* **2000**, *21*, 466–469.
(4) Fan, J.-Q. A contradictory treatment for lysosomal storage disorders: inhibitors enhance mutant enzyme activity. *Trends Pharmacol. Sci.* **2003**, *24*, 355–360.
(5) Butters, T. D. Pharmacotherapeutic strategies using small molecules for the treatment of glycolipid lysosomal storage disorders. *Expert Opin. Pharmacother.* **2007**, *8*, 427–435.
(6) Grabowski, G. A. Treatment perspectives for the lysosomal storage diseases. *Expert Opin. Emerging Drugs* **2008**, *13*, 197–211.
(7) Dvir, H.; Harel, M.; McCarthy, A. A.; Toker, L.; Silman, I.; Futerman, A. H.; Sussman, J. L. X-ray structure of human acid-beta-glucosidase, the defective enzyme in Gaucher disease. *EMBO Rep.* **2003**, *4*, 704–709.
(8) Brumshtein, B.; Wormald, M. R.; Silman, I.; Futerman, A. H.; Sussman, J. L. Structural comparison of differently glycosylated forms of acid-beta-glucosidase, the defective enzyme in Gaucher

disease. *Acta Crystallogr., Sect. D: Biol. Crystallogr.* **2006**, *62*, 1458–1465.
(9) Shaaltiel, Y.; Bartfeld, D.; Hashmueli, S.; Baum, G.; Brill-Almon, E.; Galili, G.; Dym, O.; Boldin-Adamsky, S. A.; Silman, I.; Sussman, J. L.; Futerman, A. H.; Aviezer, D. Production of glucocerebrosidase with terminal mannose glycans for enzyme replacement therapy of Gaucher's disease using a plant cell system. *Plant Biotechnol. J.* **2007**, *5*, 579–590.
(10) Brumshtein, B.; Salinas, P.; Peterson, B.; Chan, V.; Silman, I.; Sussman, J. L.; Savickas, P. J.; Robinson, G. S.; Futerman, A. H. Characterization of gene-activated human acid-{beta}-glucosidase: crystal structure, glycan composition and internalization into macrophages. *Glycobiology* **2010**, *20*, 24–32.
(11) Lieberman, R. L.; D'Aquino, J, A.; Ringe, D.; Petsko, G. A. Effects of pH and iminosugar pharmacological chaperones on lysosomal glycosidase structure and stability. *Biochemistry* **2009**, *48*, 4816–4827.
(12) Kacher, Y.; Brumshtein, B.; Boldin-Adamsky, S.; Toker, L.; Shainskaya, A.; Silman, I.; Sussman, J. L.; Futerman, A. H. Acid beta-glucosidase: insights from structural analysis and relevance to Gaucher disease therapy. *Biol. Chem.* **2008**, *389*, 1361–1369.
(13) Premkumar, L.; Sawkar, A. R.; Boldin-Adamsky, S.; Toker, L.; Silman, I.; Kelly, J. W.; Futerman, A. H.; Sussman, J. L. X-ray structure of human acid-beta-glucosidase covalently bound to conduritol-B-epoxide. Implications for Gaucher disease. *J. Biol. Chem.* **2005**, *280*, 23815–23819.
(14) Brumshtein, B.; Greenblatt, H. M.; Butters, T. D.; Shaaltiel, Y.; Aviezer, D.; Silman, I.; Futerman, A. H.; Sussman, J. L. Crystal structures of complexes of *N*-butyl- and *N*-nonyl-deoxynojirimycin bound to acid beta-glucosidase: insights into the mechanism of chemical chaperone action in Gaucher disease. *J. Biol. Chem.* **2007**, *282*, 29052–29058.
(15) Lieberman, R. L.; Wustman, B. A.; Huertas, P.; Powe, A. C., Jr.; Pine, C. W.; Khanna, R.; Schlossmacher, M. G.; Ringe, D.; Petsko, G. A. Structure of acid beta-glucosidase with pharmacological chaperone provides insight into Gaucher disease. *Nat. Chem. Biol.* **2007**, *3*, 101–107.
(16) Brumshtein, B.; Aguilar-Moncayo, M.; Garcia-Moreno, M. I.; Ortiz Mellet, C.; Garcia Fernandez, J. M.; Silman, I.; Shaaltiel, Y.; Aviezer, D.; Sussman, J. L.; Futerman, A. H. 6-Amino-6-deoxy-5,6-di-*N*-(*N*′-octyliminomethylidene)nojirimycin: synthesis, biological evaluation, and crystal structure in complex with acid beta-glucosidase. *ChemBioChem* **2009**, *10*, 1480–1485.
(17) Egido-Gabas, M.; Serrano, P.; Casas, J.; Llebaria, A.; Delgado, A. New aminocyclitols as modulators of glucosylceramide metabolism. *Org. Biomol. Chem.* **2005**, *3*, 1195–1201.
(18) Egido-Gabas, M.; Serrano, P.; Casas, J.; Zucco, M.; Emeric, G.; Llebaria, A.; Delgado, A. New aminocyclitol libraries as candidates to chemical chaperone therapy for Gaucher disease. *Naunyn-Schmiedeberg's Arch. Pharmacol.* **2007**, *374*, 340.
(19) Egido-Gabas, M.; Canals, D.; Casas, J.; Llebaria, A.; Delgado, A. Aminocyclitols as pharmacological chaperones for glucocerebrosidase, a defective enzyme in Gaucher disease. *ChemMedChem* **2007**, *2*, 992–994.
(20) Sanchez-Olle, G.; Duque, J.; Egido-Gabas, M.; Casas, J.; Lluch, M.; Chabas, A.; Grinberg, D.; Vilageliu, L. Promising results of the chaperone effect caused by iminosugars and aminocyclitol derivatives on mutant glucocerebrosidases causing Gaucher disease. *Blood Cells, Mol. Dis.* **2009**, *42*, 159–166.
(21) Serrano, P.; Casas, J.; Zucco, M.; Emeric, G.; Egido-Gabas, M.; Llebaria, A.; Delgado, A. Combinatorial approach to N-substituted aminocyclitol libraries by solution-phase parallel synthesis and preliminary evaluation as glucocerebrosidase inhibitors. *J. Comb. Chem* **2007**, *9*, 43–52.
(22) Serrano, P.; Llebaria, A.; Delgado, A. Regio- and stereoselective synthesis of aminoinositols and 1,2-diaminoinositols from conduritol B epoxide. *J. Org. Chem.* **2005**, *70*, 7829–7840.
(23) Serrano, P.; Llebaria, A.; Vazquez, J.; de Pablo, J.; Anglada, J. M.; Delgado, A. On the regio- and stereoselective synthesis of aminocyclitols from cyclitol epoxides: the effect of Li as a chelating agent. *Chem.—Eur. J.* **2005**, *11*, 4465–4472.
(24) The recovery of recombinant GlcCerase activity after thermal denaturation is currently used as an in vitro model assay for potential pharmacological chaperones (see ref 37).
(25) Rostovtsev, V. V.; Green, L. G.; Fokin, V. V.; Sharpless, K. B. A stepwise Huisgen cycloaddition process: copper(I)-catalyzed regioselective "ligation" of azides and terminal alkynes. *Angew. Chem., Int. Ed.* **2002**, *41*, 2596–2599.
(26) Gil, M. V.; Arévalo, M. J.; López, Ó. Click chemistry—What's in a name? Triazole synthesis and beyond. *Synthesis* **2007**, 1589–1620.
(27) Gonzalez-Bulnes, P.; Casas, J.; Delgado, A.; Llebaria, A. Practical synthesis of (−)-1-amino-1-deoxy-myo-inositol from achiral precursors. *Carbohydr. Res.* **2007**, *342*, 1947–1952.
(28) Inhibition constants (K_i) were only determined for compounds with IC_{50} values below 40 μM at pH 5.0 (pH for optimal enzyme activity).
(29) Only compounds **2b**, **2c**, and **3a** showed GCS inhibition (A549 cells), albeit not higher than 30% at the indicated concentration (250 μM). For a matter of comparison, a 70% inhibition of enzyme activity was found for NBDNJ at 10 μM. For experimental details, see the Supporting Information.
(30) Compounds were screened against the following glycosidases: sweet almond β-glucosidase, yeast α-glucosidase, rice α-glucosidase, rice α-galactosidase, and bovine liver β-galactosidase. For further details, see the Supporting Information.
(31) Among the most active compounds, only **1d** was nontoxic at 300 μM in wt human fibroblasts, whereas **1e** and **1f** showed CC_{50} values of 55 and 19 μM, respectively. The remaining compounds were not toxic at 300 μM, with the exceptions of **3b** and **3c**, with CC_{50} values of 97 and 170 μM, respectively. Taking the CC_{50}/K_i ratio as a measure of compound efficacy, the following values are obtained: **1c** ≥ 900; **1d** ≥ 3300; **1e** = 916; **1f** = 237.
(32) Warren, G. L.; Andrews, C. W.; Capelli, A. M.; Clarke, B.; LaLonde, J.; Lambert, M. H.; Lindvall, M.; Nevins, N.; Semus, S. F.; Senger, S.; Tedesco, G.; Wall, I. D.; Woolven, J. M.; Peishoff, C. E.; Head, M. S. A critical assessment of docking programs and scoring functions. *J. Med. Chem.* **2006**, *49*, 5912–5931.
(33) Guimaraes, C. R.; Cardozo, M. MM-GB/SA rescoring of docking poses in structure-based lead optimization. *J. Chem. Inf. Model.* **2008**, *48*, 958–970.
(34) Brik, A.; Alexandratos, J.; Lin, Y. C.; Elder, J. H.; Olson, A. J.; Wlodawer, A.; Goodsell, D. S.; Wong, C. H. 1,2,3-Triazole as a peptide surrogate in the rapid synthesis of HIV-1 protease inhibitors. *ChemBioChem* **2005**, *6*, 1167–1169.
(35) Appendino, G.; Bacchiega, S.; Minassi, A.; Cascio, M. G.; De Petrocellis, L.; Di Marzo, V. The 1,2,3-triazole ring as a peptido- and olefinomimetic element: discovery of click vanilloids and cannabinoids. *Angew. Chem., Int. Ed.* **2007**, *46*, 9312–9315.
(36) Odlo, K.; Hentzen, J.; dit Chabert, J. F.; Ducki, S.; Gani, O. A.; Sylte, I.; Skrede, M.; Florenes, V. A.; Hansen, T. V. 1,5-Disubstituted 1,2,3-triazoles as cis-restricted analogues of combretastatin A-4: synthesis, molecular modeling and evaluation as cytotoxic agents and inhibitors of tubulin. *Bioorg. Med. Chem.* **2008**, *16*, 4829–4838.
(37) Sawkar, A. R.; Cheng, W. C.; Beutler, E.; Wong, C. H.; Balch, W. E.; Kelly, J. W. Chemical chaperones increase the cellular activity of N370S beta-glucosidase: a therapeutic strategy for Gaucher disease. *Proc. Natl. Acad. Sci. U.S.A.* **2002**, *99*, 15428–15433.
(38) *Maestro*, version 8.5; Schrödinger, LLC: New York, 2008.
(39) *MacroModel*, version 9.6; Schrödinger, LLC: New York, 2005.
(40) Jorgensen, W. L.; Maxwell, D. S.; TiradoRives, J. Development and testing of the OPLS all-atom force field on conformational energetics and properties of organic liquids. *J. Am. Chem. Soc.* **1996**, *118*, 11225–11236.
(41) Still, W. C.; Tempczyk, A.; Hawley, R. C.; Hendrickson, T. Semianalytical treatment of solvation for molecular mechanics and dynamics. *J. Am. Chem. Soc.* **1990**, *112*, 6127–6129.
(42) *Glide*, version 5.0; Schrödinger, LLC: New York, 2008.
(43) Friesner, R. A.; Banks, J. L.; Murphy, R. B.; Halgren, T. A.; Klicic, J. J.; Mainz, D. T.; Repasky, M. P.; Knoll, E. H.; Shelley, M.; Perry, J. K.; Shaw, D. E.; Francis, P.; Shenkin, P. S. Glide: a new approach for rapid, accurate docking and scoring. 1. Method and assessment of docking accuracy. *J. Med. Chem.* **2004**, *47*, 1739–1749.
(44) Halgren, T. A.; Murphy, R. B.; Friesner, R. A.; Beard, H. S.; Frye, L. L.; Pollard, W. T.; Banks, J. L. Glide: a new approach for rapid, accurate docking and scoring. 2. Enrichment factors in database screening. *J. Med. Chem.* **2004**, *47*, 1750–1759.
(45) Friesner, R. A.; Murphy, R. B.; Repasky, M. P.; Frye, L. L.; Greenwood, J. R.; Halgren, T. A.; Sanschagrin, P. C.; Mainz, D. T. Extra precision glide: docking and scoring incorporating a model of hydrophobic enclosure for protein−ligand complexes. *J. Med. Chem.* **2006**, *49*, 6177–6196.
(46) Klicic, J. J.; Friesner, R. A.; Liu, S. Y.; Guida, W. C. Accurate prediction of acidity constants in aqueous solution via density functional theory and self-consistent reaction field methods. *J. Phys. Chem. A* **2002**, *106*, 1327–1335.
(47) *Jaguar*, version 7.5; Schrödinger, LLC: New York, 2008.
(48) Berman, H. M.; Westbrook, J.; Feng, Z.; Gilliland, G.; Bhat, T. N.; Weissig, H.; Shindyalov, I. N.; Bourne, P. E. The Protein Data Bank. *Nucleic Acids Res.* **2000**, *28*, 235–242.
(49) *LigPrep*, version 2.2; Schrödinger, LLC: New York, 2005.
(50) *Molecular Operating Environment*, version 2008.10; Chemical Computing Group: Montreal, Quebec, Canada, 2008.